Turkish Journal of Medical Sciences

Volume 47 | Number 5 Article 30

1-1-2017

Evaluation of pulmonary vein anatomy using 256-slice computed tomography

YINGHONG SHI

SHAOHUA MI

YUNXIA SHI

HONGBO WANG

JIAN LI

See next page for additional authors

Evaluation of pulmonary vein anatomy using 256-slice computed tomography

Authors
YINGHONG SHI, SHAOHUA MI, YUNXIA SHI, HONGBO WANG, JIAN LI, BENXIA YU, FENGLI LIU, HENG MA, and BIN WANG

TÜBİTAK

Turkish Journal of Medical Sciences

http://journals.tubitak.gov.tr/medical/

Research Article

Turk J Med Sci
(2017) 47: 1526-1534

doi:10.3906/sag-1506-84

Evaluation of pulmonary vein anatomy using 256-slice computed tomography

Yinghong SHI[1], Shaohua MI[2], Yunxia SHI[1], Hongbo WANG[1], Jian LI[1], Benxia YU[1], Fengli LIU[1], Heng MA[1], Bin WANG[3,*]

[1]Department of Radiology, Yuhuangding Hospital, Yantai, Shandong, P.R. China
[2]Department of Cardiology, Yuhuangding Hospital, Yantai, Shandong, P.R. China
[3]Medical Imaging Research Institute, Binzhou Medical University, Yantai, Shandong, P.R. China

Received: 18.06.2015 • **Accepted/Published Online:** 09.06.2017 • **Final Version:** 13.11.2017

Background/aim: This study aimed to evaluate pulmonary vein (PV) anatomy using 256-slice computed tomography (CT), which may be necessary for electrophysiologists to know before radiofrequency catheter ablation (RFCA) therapy.

Materials and methods: A total of 102 patients with paroxysmal and persistent atrial fibrillation underwent 256-slice cardiac CT angiography prior to catheter ablation. PV morphology, ostial diameter, ostial orientation, and distance from ostium to first bifurcation were evaluated using three-dimensional volume-rendering and multiplanar-reformatting technology.

Results: We found that 72.5% of patients had four conventional PVs. On the right, 22.5% of patients had one accessory PV, 4.9% had 2 accessory PVs, 1% had one common PV, and 1% had one top vein. On the left, 27.5% of patients had one common PV. Additionally, 9.8% of patients had bilateral PV variation. Ostial size was larger for superior PVs than inferior PVs and larger for right PVs than left PVs. PV ostia on the right tended to be more circular. There was a rather wide variation of projective angle and distance from ostium to first bifurcation. Early branching occurred more often in the right inferior PV.

Conclusion: 256-Slice CT can depict PV anatomy and afford substantial data, which will help electrophysiologists conduct the RFCA procedure safely and efficiently.

Key words: Pulmonary vein, computed tomography, radiofrequency catheter ablation

1. Introduction

For patients with atrial fibrillation (AF) originating in the pulmonary veins (PVs), radiofrequency catheter ablation (RFCA) is an effective and safe treatment method (1–3). Because PVs display variable morphology, ostial diameter, ostial orientation, and distance from ostium to first bifurcation, familiarity with PV anatomy prior to RFCA may be necessary for electrophysiologists to map precisely, select proper catheter size, target the ablation points, and reduce procedure time and radiation exposure (4,5).

MR angiography (MRA) and multislice spiral computed tomography angiography (MSCTA) are noninvasive imaging modalities, which appear to provide similar and detailed anatomic and quantitative information before RFCA of AF (6). The advantages of MRA/CTA are as follows: imaging the anatomy of PVs and left atrium (LA) preprocedurally; assessing the relationship between the LA and adjacent structures; understanding the morphological remodeling of PVs and LA; and detecting complications (7).

However, long scan time, high expense, and contraindications (including implanted electronic devices and claustrophobia) limit MRA utility. Previous studies using 4-, 16-, and 64-row CT demonstrated that MSCTA can visualize the anatomy of the PV system (8–12). Radiation exposure is their main risk.

The development of wide-area coverage multidetector CT, such as the 256-slice and 320-row CT scanners, makes it possible to better visualize PV anatomy. These scanners offer the advantage of eliminating stair-step and misalignment artifacts, lowering radiation dose, and reducing intravenous contrast requirement (13). A recent study using low-dose, 320-row CT showed the technical feasibility for PV imaging (14). However, this study did not depict PV anatomy.

To date, no studies have evaluated PV anatomy using 256-slice CT. Therefore, the purpose of our study is to establish PV morphology, ostial diameter, ostial orientation, and distance from ostium to first bifurcation for patients with AF using 256-slice CT.

* Correspondence: binwangyt001@163.com

2. Materials and methods

2.1. Patients

This study consisted of retrospective data collection and analysis of consecutive patients scheduled to undergo catheter ablation for paroxysmal and persistent AF from June 2013 to December 2014. All patients underwent cardiac CTA within 3 days before the ablation procedure with a 256-slice CT scanner. Patients with renal insufficiency, allergy to iodine-containing contrast medium, unstable clinical condition, or inability to follow breath-holding instructions were excluded from the study.

The study population consisted of 102 patients (46 males, age range 34–76 years, mean 56; 56 females, 24–72 years, mean 55).

The study was approved by the Institution Ethics Board of Yuhuangding Hospital, Yantai, China. Our institutional review board waived the need for written informed consent from the participants, because it was a retrospective review of PV angiography performed before catheter ablation.

2.2. Radiology method

All patients underwent a retrospectively ECG-gated cardiac CT examination using 256-slice CT technology (Brilliance iCT; Philips, Cleveland, OH, USA). The scan parameters were as follows: tube voltage, 100 kVp; effective tube current–time product, 700 mAs; pitch, 0.18; detector collimation, 128 × 0.625 mm; rotation time, 270 ms; slice thickness, 0.9 mm; increment, 0.6 mm; effective radiation dose (ED), 6.35–10.92 mSv. No additional β-blocker was performed prior to CTA. The scan coverage was planned from the level of the tracheal bifurcation to the diaphragm. Data were acquired in the craniocaudal direction.

Automatic bolus tracking (Bolus Pro; Philips) was used by defining a region of interest (ROI) in the ascending aorta at the level of aortopulmonary fenestration. The scan was initiated 6 s after the signal attenuation had reached a predetermined threshold of 180 Hounsfield units (HU).

Nonionic contrast medium (average 75 mL) (Ultravist 370, Bayer Schering Pharma AG, Berlin, Germany) was injected into the antecubital vein through a 20-gauge catheter at a rate of 5 mL/s using a dual-head injector.

2.3. View of PV morphology: measurement of ostial diameter, projective angle, and distance from ostium to first bifurcation

Raw spiral CT data were reconstructed at 45% of the RR interval (maximum LA dilated), postprocessed, and analyzed on a dedicated workstation (IntelliSpace Portal, Philips).

The PV ostium was the atriopulmonary venous junction. In epicardial views, it was identified as the point of reflection of the parietal pericardium from the LA. Conventional PV anatomy was defined as the presence of single right and left superior and inferior PVs that drained into the LA without any accessory veins (Figure 1A). Accessory PVs were defined as extra veins with independent atriopulmonary venous junctions, separate from the superior and inferior PVs and named after the pulmonary lobe or segment that they drained (15) (Figure 1B). The top vein was defined as the accessory PV that entered the roof of the LA (Figure 1C). A common vein occurred when superior and inferior PVs combined proximal to the LA, resulting in only one atriopulmonary venous junction on the involved side (Figure 1D). Early branching was defined as the branching of PV within 5 mm of the atriopulmonary venous junctions.

PV morphology was analyzed using three-dimensional volume-rendering (VR) technology. Virtual endoscopy was used when it was difficult to distinguish a common PV.

Ostial diameter, projective angle, and distance from ostium to first bifurcation were measured using multiplanar-reformatting (MPR) technology.

The anterior–posterior (AP) diameter, superior–inferior (SI) diameter, and cross-sectional area of the PV ostia were measured on the third orthogonal plane (double-oblique plane) (Figure 2).

PV ovality was then assessed using an ostium index (AP diameter/SI diameter). A ratio closer to 1.0 would imply a more circular vein.

The projective angles of PVs to the coronary plane were measured on the transverse image (Figure 3A). Similarly, the projective angles of PVs to the transverse plane were measured on the coronary image (Figure 3B).

All images were interpreted in consensus by two independent radiologists, both of whom had more than 5 years of cardiothoracic CT experience.

2.4. Statistics

SPSS 17.0 was used to perform the statistical analysis. Descriptive statistics were used, and data were given as mean ± standard deviation. An unpaired Student's t-test was used to compare PVs for ostial diameter, projective angle, and distance from ostium to first bifurcation. Statistical significance was assigned at $P < 0.05$.

3. Results

Cardiac CT scanning was successfully performed for all 102 subjects, and PVs were clearly shown in the images.

3.1. PV morphology

The total number and percentages of conventional and variant PVs are summarized in Table 1.

Ten (9.8%) patients had bilateral PV anomalies (Figure 1D). No anomalous PVs drained blood from the lung into the systemic circulation.

3.2. PV ostial diameters/indices

The mean AP, SI diameter, cross-sectional area, and ostium index values are shown in Table 2.

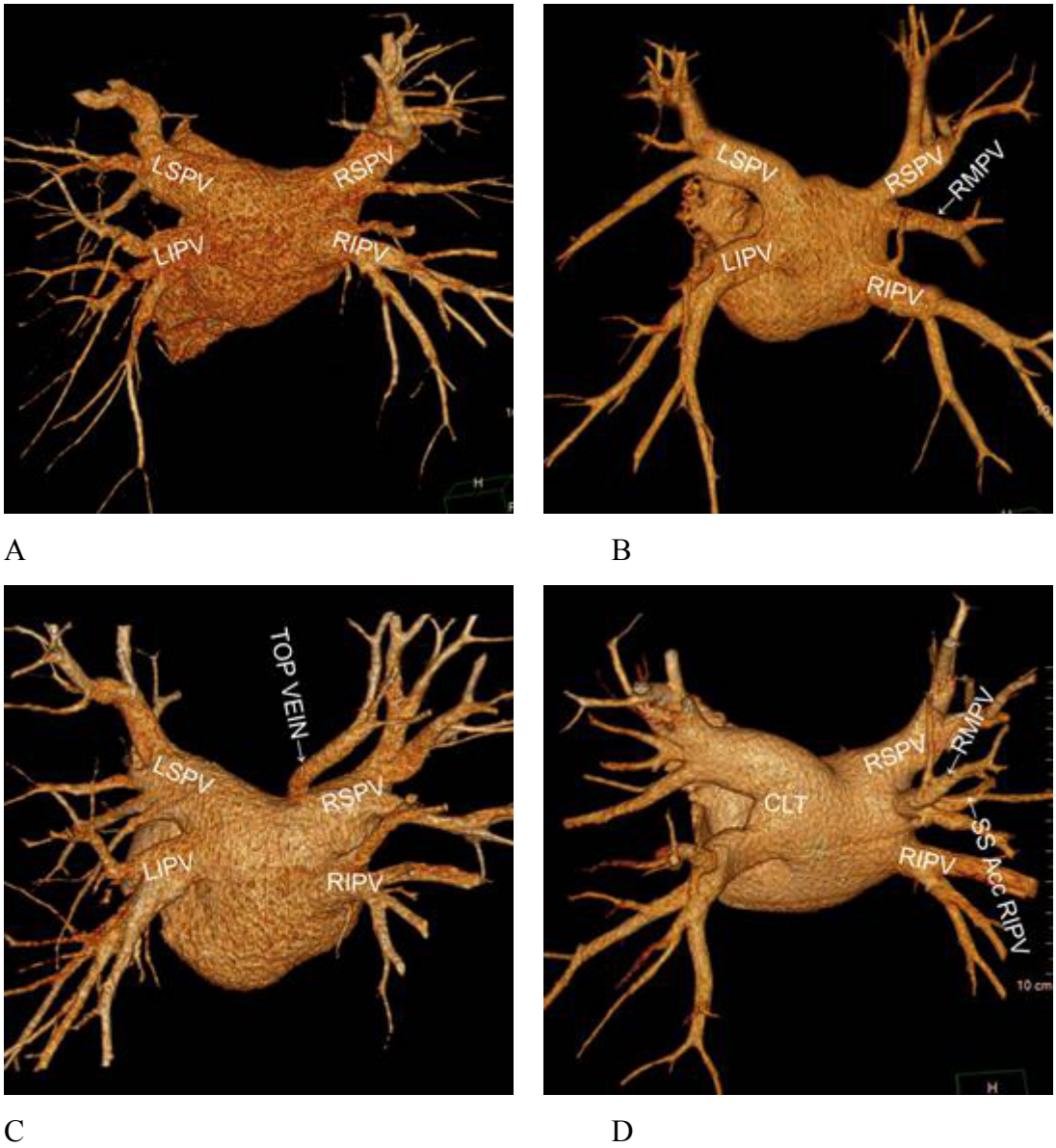

Figure 1. Pulmonary vein morphology. A) Conventional pulmonary veins: RSPV, right superior pulmonary vein; RIPV, right inferior pulmonary vein; LSPV, left superior pulmonary vein; LIPV, left inferior pulmonary vein. B) RMPV, right middle lobe pulmonary vein. C) Right top vein. D) Two accessory pulmonary vein on the right: RMPV and SS Acc. RIPV, superior segment of the right lower lobe accessory pulmonary vein; common left trunk on the left.

Ostial AP, SI diameter, and area were larger for superior PVs than inferior PVs (all $P < 0.05$); however, AP diameter was not significantly larger for RSPV than RIPV ($P > 0.05$). Ostial AP, SI diameter, and area were larger for right PVs than left PVs (all $P < 0.05$); however SI diameter was not significantly larger for RIPV than LIPV ($P > 0.05$).

The ostial AP diameter of the common left trunk (CLT) was shorter than that of the right PVs; however, there was no statistical significance (all $P > 0.05$). The ostial AP diameter of CLT was larger than that of the left PVs (all $P < 0.05$). The ostial SI diameter and area of CLT were larger than those of the four main veins (all $P < 0.05$).

Ostial AP, SI diameter, and area of RMPV were less than those of the four main veins (all $P < 0.05$).

The mean SI diameter for each type of vein was larger than the mean AP diameter (all $P < 0.05$), except for RMPV. The ostial index of RSPV, RIPV, and RMPV was larger than that of the left PVs (all $P < 0.05$), and the superior and inferior PVs and RMPV ostia on the right tended to be more circular. The ostial index of CLT was smaller

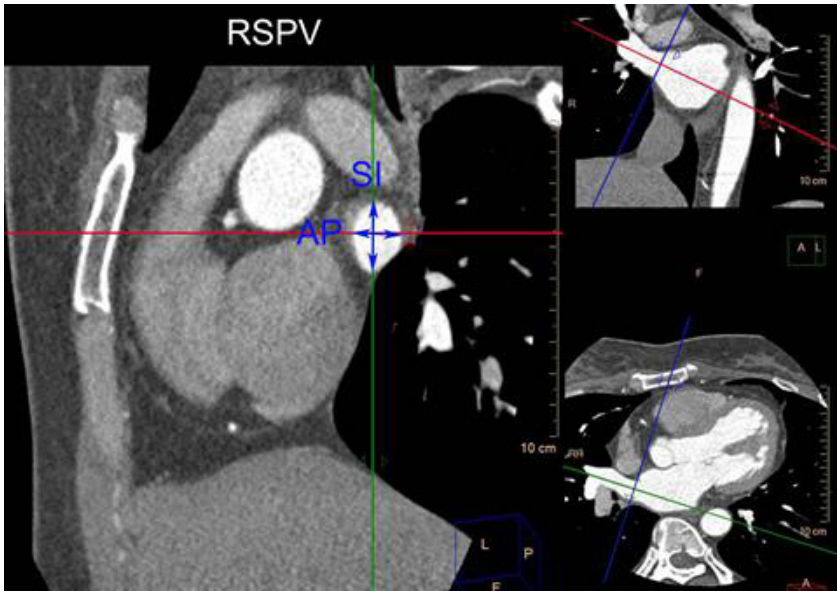

Figure 2. Measurements of AP, SI diameter, and cross-sectional area of RSPV ostium on the third orthogonal plane (double-oblique plane).

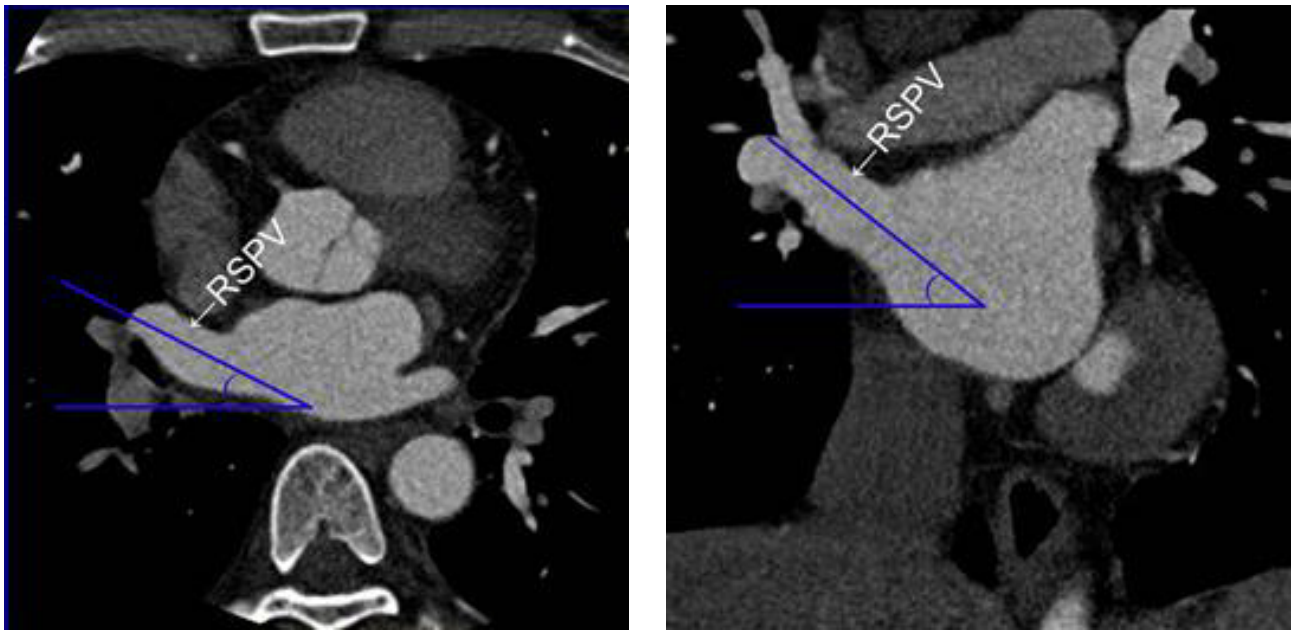

A B

Figure 3. A) Projective angle of RSPV to the coronary plane; B) projective angle of RSPV to the transversal plane.

than that of the right and left PVs (all $P < 0.05$), and the common left ostia tended to have a more oval shape.

3.3. Ostial orientation

The mean projective angles to coronary and transverse planes are given in Table 3.

Both superior PVs bent forward and upward, whereas both inferior PVs directed backward and downward. There was a rather wide variation of PV directions.

There were greater variations in the projective angles to coronary planes of inferior PVs compared with superior PVs, and left PVs compared with right PVs. Variations of the projective angles to coronary planes of CLT and RMPV were larger than those of RSPV, although they were smaller than those of RIPV, LSPV, and LIPV.

There were greater variations in the projective angles to the transverse plane of superior PVs compared with

Table 1. Number and percentage of PV variations.

PV	No./%			
Conventional four PV	74/72.5%			
Variant PV	Accessory PV (29/28.4%)			Common PV (29/28.4%)
	R	RMPV	19/18.6%	1/1%
		SS Acc. RIPV	4/3.9%	
		Top vein	1/1%	
		RMPV+ SS Acc. RIPV	5/4.9%	
	L	0/0		28/27.5%

PV: Pulmonary vein; RMPV: right middle lobe pulmonary vein; SS Acc. RIPV: superior segment of the right lower lobe accessory pulmonary vein.

Table 2. PV ostial diameters/indices.

PVs	AP diameter (mm)	SI diameter (mm)	Cross-sectional area (mm^2)	Ostium index (AP/SI)
Right PVs				
Superior (101)	16.81 ± 3.59	22.89 ± 5.19	294.13 ± 110.45	0.75 ± 0.15
Inferior (101)	16.33 ± 5.16	17.62 ± 4.24	215.32 ± 101.03	0.94 ± 0.24
Left PVs				
Superior (74)	12.68 ± 2.41	21.49 ± 4.26	203.21 ± 75.03	0.60 ± 0.12
Inferior (74)	11.69 ± 2.48	17.41 ± 2.89	153.10 ± 46.29	0.65 ± 0.28
Common PVs				
R (1)	19.10	30.20	445.20	0.63
L (28)	15.52 ± 5.07	34.16 ± 6.55	410.25 ± 125.50	0.43 ± 0.13
Accessory PVs				
RMPV (24)	8.30 ± 2.27	8.36 ± 1.63	51.94 ± 21.87	0.86 ± 0.11
SS Acc. RIPV (9)	9.34 ± 3.35	8.64 ± 1.80	65.26 ± 39.63	0.85 ± 0.13
Right top vein (1)	3.60	5.70	14.90	0.63
L(0)				

Data are shown as mean ± standard deviation.
PV: Pulmonary vein; RMPV: right middle lobe pulmonary vein; SS Acc. RIPV: superior segment of the right lower lobe accessory pulmonary vein; AP: anterior-posterior; SI: superior-inferior.

inferior PVs, and right PVs compared with left PVs. The variation of the projective angle to the transverse plane of CLT was larger than those of superior PVs, but smaller than those of inferior PVs. The variation of the projective angle to the transverse plane of RMPV was larger than those of the main four PVs.

3.4. Distance from ostium to first bifurcation

The mean distance values from ostium to first bifurcation are shown in Table 3.

Distances from ostium to first bifurcation were larger for superior PVs than inferior PVs, and larger for left PVs than right PVs (all $P < 0.05$). The distance from ostium to first bifurcation of CLT was statistically smaller than that of RSPV, LSPV, LIPV, and RMPV ($P < 0.05$), but larger than that of RIPV ($P < 0.05$). The distance from ostium to first bifurcation of RMPV was statistically larger than that of RSPV, RIPV, LIPV, and CLT ($P < 0.05$), but smaller than that of LSPV ($P < 0.05$). The distance from ostium to first bifurcation of RIPV was the shortest of the PVs.

Table 3. Projective angles to coronary and transverse plane and distance from ostium to first bifurcation of PVs.

PVs	Project angle to coronary plane (°)	Project angle to transverse plane (°)	Distance from ostium to first bifurcation (mm)
Right PVs			
Superior (101)	24.26 ± 8.18	30.33 ± 10.72	12.74 ± 6.03
Inferior (101)	21.72 ± 11.22	17.21 ± 11.81	5.03 ± 3.70
Left PVs			
Superior (74)	13.57 ± 7.14	25.56 ± 7.38	17.93 ± 4.86
Inferior (74)	17.79 ± 11.98	22.20 ± 12.38	13.42 ± 5.15
Common PVs			
R (1)	11.10	0.00	7.60
L (28)	22.51 ± 9.69	25.52 ± 11.53	9.49 ± 2.89
Accessory PVs			
RMPV (24)	27.43 ± 12.63	14.75 ± 14.62	15.32 ± 6.99
SS Acc. RIPV (9)	42.46 ± 18.48	24.50 ± 9.45	9.04 ± 3.80
Right top vein (1)	10.80	36.70	10.00
L (0)			

Data are shown as mean ± standard deviation.
PV: Pulmonary vein; RMPV: right middle lobe pulmonary vein; SS Acc. RIPV: superior segment of the right lower lobe accessory pulmonary vein.

LSPVs have no early branching, LIPVs have 3 (4.1%) early branchings, RSPVs have 9 (8.9%) early branchings, RIPVs have 58 (57.4%) early branchings, and RMPVs have 3 (10.7%) early branchings.

4. Discussion

Our study used 256-slice CT to evaluate PV anatomy and confirmed that it was substantially variable.

First, PV morphology was analyzed. The results support previous ideas that PV anatomy is commonly variable (8,11,16–20). The right side tends to be complex, often having one or more accessory veins, whereas the left side tends to be simplified, often having common veins, which rarely occur on the right. Some newly named PV variants were found in a consecutive large series of patients with AF or not (20). Contradictory suggestions have been made about whether the prevalence of accessory PV is significantly different from common PV or not. Chen et al. suggested that RMPV was the most common variant (20), and Kanaji et al. found that the most common variant was a common PV (21). However, our study found that the prevalence of accessory PV is equal to common PV. Any anatomical variant could be arrhythmogenic and associated with the occurrence of AF. Accessory PVs and common ostia were identified as possible reasons for incomplete ablation (22,23). Therefore, carefully recognizing variant PVs prior to ablation maximizes the efficacy of the procedure.

Second, our study measured AP, SI diameter, area, and ostial index of PVs, leading to the following five points: ostial sizes of superior PVs are larger than those of inferior PVs; ostial sizes of right PVs are larger than those of left PVs; the ostial size of CLT is the largest; the ostial size of RMPV is the smallest; and superior PV, inferior PV, and RMPV ostia on the right tend to be more circular, whereas left common ostia tend to have a more oval shape. These five points are consistent with previous studies (8,11,16,20), but afford more information. PV ostial size facilitated the selection of the size of catheters and selection of appropriate energy to avoid stenosis. An oval-shaped ostium may affect the position and stability of a circular catheter (1). Therefore, more attention should be paid to CLT with a more oval-shape ostium. Kanaji et al. reported that no patient had a catheter lodged in accessory PVs, presumably due to the recognition of the specific anatomy before the ablation procedure (21). Advanced knowledge of the PV variant maximizes the safety of the procedure.

Third, our study shows the mean projective angles of PVs. For each PV, there is a rather wide variation of PV directions. There is a subtle difference between our measurements and those of previous studies (10,16,20,24). Additionally, our study measured the projective angles of RMPV and CLT, which had not been measured in previous studies. The projective angle is the stable imaging anatomic structure of PVs, which does not differ among patients suffering from AF or not (10). Electrophysiologists can adjust the angles of the central X-ray according to these projective angles and improve the conventional method to reduce the procedure time of fluoroscopy.

Fourth, our study shows greater variation in the distance between the ostium and the first bifurcation than in the diameter. The LSPV tends to have a longer trunk, the RIPV tends to have a shorter trunk, and the RIPV tends to have an earlier branching, which is in line with previous studies (8,16). However, the distance of RMPV in our study is larger than in Cronin et al.'s study, which shows great variation in PV length. Pulmonary vein narrowing after RFCA seems to be critically dependent on catheter position instead of duration of radiofrequency energy application (25). Thus, more attention should be paid to early branching to avoid ablation and damage.

Tekbas et al. (26) used 64-row CT to classify the RMPV as indirect drainage and direct drainage. Subsegmental classification has no importance for the exact ablation procedures, although the number of the atrial ostia is an important factor. Our study evaluated 24 cases of RMPVs draining to the LA directly and found great variation in RMPV anatomy.

A 256-slice CT is a 128 × 0.625-mm detector row system with a dual focal spot, which makes it possible to cover the cardiac anatomy in one or two steps. Only the narrow overlap zone between the two steps is kept to ensure the continuity of images. The gantry rotation time is 270 ms, translating to an approximate temporal resolution of 135 ms. Iterative reconstruction can effectively reduce radiation dose and improve image quality (27). These properties enable iCT to reduce the scanning time, duration of breath-holding, motion artifacts, contrast medium requirements, and radiation dose (13,28). Radiation exposure is a reason for concern. The ED in our scanning with 256-slice CT is 6.35–10.92 mSv, which is relatively lower compared to the older generation of MSCT (29).

Retrospective ECG gating has been previously performed in LA and PV imaging (11,15,30) and has been used successfully in our study. It is an important factor that affects the radiation dose. Compared with retrospective scanning, prospective ECG gating allows the X-ray beams to be turned on during preselected phases in the cardiac cycles and obviously reduces radiation dose while maintaining equivalent diagnostic accuracy and comparable image quality (31,32). However, it was limited to patients with a heart rate below 75 bpm, and the image quality at this heart rate was decreased, which cannot be comparable to retrospective ECG gating (31).

Our study has several limitations. We did not modulate tube voltage based on body mass index. We did not focus on contrast volumes, although the use of 100 kV facilitated a reduction in the contrast volumes without a compromise in image quality (33). Lastly, we had no diagnostic standard for comparison with our CT data, because the PV anatomy is complex. Cross-sectional imaging techniques, such as CT or MR imaging combined with MPR or 3D capabilities, should best depict PV anatomy (34).

In conclusion, 256-slice CT allows precise visualization of the PV morphology, ostial diameter, ostial orientation, and distance from ostium to first bifurcation, which may be of great help for electrophysiologists to become familiar with PVs and carry out the RFCA procedure safely and efficiently.

Acknowledgments

This work was supported by the Shandong Province Natural Science Foundation (ZR2012HM013) and the Yantai City Science and Technology Development Plan (2012090).

References

1. Pappone C, Rosanio S, Oreto G, Tocchi M, Gugliotta F, Vicedomini G, Salvati A, Dicandia C, Mazzone P, Santinelli V et al. Circumferential radiofrequency ablation of pulmonary vein ostia: a new anatomic approach for curing atrial fibrillation. Circulation 2000; 102: 2619-2628.
2. Oral H, Knight BP, Tada H, Ozaydin M, Chugh A, Hassan S, Scharf C, Lai SW, Greenstein R, Pelosi F Jr et al. Pulmonary vein isolation for paroxysmal and persistent atrial fibrillation. Circulation 2002; 105: 1077-1081.
3. Zheng YF, Yang D, John M, Comaniciu D. Multi-part modeling and segmentation of left atrium in C-arm CT for image-guided ablation of atrial fibrillation. IEEE T Med Imag 2014; 33: 318-331.
4. Lin WS, Prakash VS, Tai CT, Hsieh MH, Tsai CF, Yu WC, Lin YK, Ding YA, Chang MS, Chen SA. Pulmonary vein morphology in patients with paroxysmal atrial fibrillation initiated by ectopic beats originating from the pulmonary veins: implications for catheter ablation. Circulation 2000; 101: 1274-1281.

5. Kistler PM, Rajappan K, Jahngir M, Earley MJ, Harris S, Abrams D, Gupta D, Liew R, Ellis S, Sporton SC et al. The impact of CT image integration into an electroanatomic mapping system on clinical outcomes of catheter ablation of atrial fibrillation. J Cardiovasc Electrophysiol 2006; 17: 1093-1101.
6. Hamdan A, Charalampos K, Roettgen R, Wellnhofer E, Gebker R, Paetsch I, Jahnke C, Schnackenburg B, Tang M, Gerds-Li H et al. Magnetic resonance imaging versus computed tomography for characterization of pulmonary vein morphology before radiofrequency catheter ablation of atrial fibrillation. Am J Cardiol 2009; 104: 1540-1546.
7. Wazni OM, Tsao HM, Chen SA, Chuang HH, Saliba W, Natale A, Klein AL. Cardiovascular imaging in the management of atrial fibrillation. J Am Coll Cardiol 2006; 48: 2077-2084.
8. Cronin P, Kelly AM, Desjardins B, Patel S, Gross BH, Kazerooni EA, Morady F, Oral H, Carlos RC. Normative analysis of pulmonary vein drainage patterns on multidetector CT with measurements of pulmonary vein ostial diameter and distance from ostium to first bifurcation. Acad Radiol 2007; 14: 178-188.
9. Kaseno K, Tada H, Koyama K, Jingu M, Hiramatsu S, Yokokawa M, Goto K, Naito S, Oshima S, Taniguchi K. Prevalence and characterization of pulmonary vein variants in patients with atrial fibrillation determined using 3-dimensional computed tomography. Am J Cardiol 2008; 101: 1638-1642.
10. Wang J, Zhang Z, Yu W, Miao C, Yan Z, Zhao Y. A study of images of projective angles of pulmonary veins. Eur J Radiol 2009; 71: 474-479.
11. Thorning C, Hamady M, Liaw JV, Juli C, Lim PB, Dhawan R, Peters NS, Davies DW, Kanagaratnam P, O'Neill MD et al. CT evaluation of pulmonary venous anatomy variation in patients undergoing catheter ablation for atrial fibrillation. Clin Imag 2011; 35: 1-9.
12. Manghat NE, Mathias HC, Kakani N, Hamilton MC, Morgan-Hughes G, Roobottom CA. Pulmonary venous evaluation using electrocardiogram-gated 64-detector row cardiac CT. Br J Radiol 2012; 85: 965-971.
13. Hsiao EM, Rybicki FJ, Steigner M. CT Coronary angiography: 256-slice and 320-detector row scanners. Curr Cardiol Rep 2010; 12: 68-75.
14. Yang L, Xu L, Yan Z, Yu W, Fan Z, Lv B, Zhang Z. Low dose 320-row CT for left atrium and pulmonary veins imaging—the feasibility study. Eur J Radiol 2012; 81: 1549-1554.
15. Lacomis JM, Wigginton W, Fuhrman C, Schwartzman D, Armfield DR, Pealer KM. Multi-detector row CT of the left atrium and pulmonary veins before radio-frequency catheter ablation for atrial fibrillation. Radiographics 2003; 23: S35-48.
16. Chu ZG, Gao HL, Yang ZG, Yu JQ, Deng W, Wang QL, Peng LQ, Dong ZH. Pulmonary veins of the patients with atrial fibrillation: dual-source computed tomography evaluation prior to radiofrequency catheter ablation. Int J Cardiol 2011; 148: 245-248.
17. Ghaye B, Szapiro D, Dacher JN, Rodriguez LM, Timmermans C, Devillers D, Dondelinger RF. Percutaneous ablation for atrial fibrillation: the role of cross-sectional imaging. Radiographics 2003; 23: S19-33.
18. Marom EM, Herndon JE, Kim YH, McAdams HP. Variations in pulmonary venous drainage to the left atrium: implications for radiofrequency ablation. Radiology 2004; 230: 824-829.
19. Wannasopha Y, Oilmungmool N, Euathrongchit J. Anatomical variations of pulmonary venous drainage in Thai people: multidetector CT study. Biomed Imag Interv J 2012; 8: e4.
20. Chen J, Yang ZG, Xu HY, Shi K, Long QH, Guo YK. Assessments of pulmonary vein and left atrial anatomical variants in atrial fibrillation patients for catheter ablation with cardiac CT. Eur Radiol 2017; 27: 660-670.
21. Kanaji Y, Miyazaki S, Iwasawa J, Ichihara N, Takagi T, Kuroi A, Nakamura H, Taniguchi H, Hachiya H, Iesaka Y. Pre-procedural evaluation of the left atrial anatomy in patients referred for catheter ablation of atrial fibrillation. J Cardiol 2016; 67: 115-121.
22. Tsao HM, Wu MH, Yu WC, Tai CT, Lin YK, Haieh MH, Ding YA, Chang MS, Chen SA. Role of right middle pulmonary vein in patients with paroxysmal atrial fibrillation. J Cardiovasc Electrophysiol 2001; 12: 1353-1357.
23. Schwartzman D, Bazaz R, Nosbisch J. Common left pulmonary vein: a consistent source of arrhythmogenic atrial ectopy. J Cardiovasc Electrophysiol 2004; 15: 560-566.
24. Van der Voort PH, Van den Bosch H, Post JC, Meijer A. Determination of the spatial orientation and shape of pulmonary vein ostia by contrast-enhanced magnetic resonance angiography. Europace 2006; 8: 1-6.
25. Scharf C, Sneider M, Case I, Chugh A, Lai SW, Pelosi F Jr, Knight BP, Kazerooni E, Morady F, Oral H. Anatomy of the pulmonary veins in patients with atrial fibrillation and effects of segmental ostial ablation analyzed by computed tomography. J Cardiovasc Electrophysiol 2003; 14: 150-155.
26. Tekbas G, Ekici F, Tekbas E, Gumus H, Onder H, Bilici A, Yavuz C, Hamidi C. Evaluation of pulmonary vein variations in the middle pulmonary lobe with 64-slice multidetector computed tomography. Eur Rev Med Pharmacol Sci 2011; 15: 1395-1400.
27. Miéville FA, Gudinchet F, Brunelle F, Bochud FO, Verdun FR. Iterative reconstruction methods in two different MDCT scanners: physical metrics and 4-alternative forced-choice detectability experiments—a phantom approach. Phys Med 2013; 29: 99-110.
28. Klass O, Walker M, Siebach A, Stuber T, Feuerlein S, Juchems M, Hoffmann MH. Prospectively gated axial CT coronary angiography: comparison of image quality and effective radiation dose between 64- and 256-slice CT. Eur Radiol 2010; 20: 1124-1131.

29. Schroeder S, Achenbach S, Bengel F, Burgstahler C, Cademartiri F, de Feyter P, George R, Kaufmann P, Kopp AF, Knuuti J et al. Cardiac computed tomography: indications, applications, limitations, and training requirements: report of a writing group deployed by the Working Group Nuclear Cardiology and Cardiac CT of the European Society of Cardiology and the European Council of Nuclear Cardiology. Eur Heart J 2008; 29: 531-556.

30. Lacomis JM, Goitein O, Deible C, Schwartzman D. CT of the pulmonary veins. J Thorac Imag 2007; 22: 63-76.

31. Hou Y, Yue Y, Guo WL, Feng Gq, Yu T, Li GW, Vembar M, Olszewski ME, Guo QY. Prospectively versus retrospectively ECG-gated 256-slice coronary CT angiography: image quality and radiation dose over expanded heart rates. Int J Cardiovasc Imag 2012; 28: 153-162.

32. Menke J, Unterberg-Buchwald C, Staab W. Head-to-head comparison of prospectively triggered vs retrospectively gated coronary computed tomography angiography: meta-analysis of diagnostic accuracy, image quality, and radiation dose. Am Heart J 2013; 165: 154-163.

33. Stolzmann P, Leschka S, Scheffel H, Krauss T, Desbiolles L, Plass A, Genoni M, Flohr TG, Wildermuth S, Marincek B et al. Dual-source CT in step-and-shoot mode: noninvasive coronary angiography with low radiation dose. Radiology 2008; 249: 71-80.

34. Kim YH, Marom EM, Herndon JE 2nd, McAdams HP. Pulmonary vein diameter, cross-sectional area, and shape: CT analysis. Radiology 2005; 235: 43-50.